Journal of Biomedical Optics

BiomedicalOptics.SPIEDigitalLibrary.org

High-speed spatial frequency domain imaging with temporally modulated light

Matthew B. Applegate
Darren Roblyer

SPIE.

Matthew B. Applegate, Darren Roblyer, "High-speed spatial frequency domain imaging with temporally modulated light," *J. Biomed. Opt.* **22**(7), 076019 (2017), doi: 10.1117/1.JBO.22.7.076019.

Journal of Biomedical Optics 22(7), 076019 (July 2017)

High-speed spatial frequency domain imaging with temporally modulated light

Matthew B. Applegate and Darren Roblyer*
Boston University, Department of Biomedical Engineering, Boston, Massachusetts, United States

Abstract. Spatial frequency domain imaging (SFDI) is a wide-field diffuse optical technique used to obtain optical properties and chromophore concentrations in highly scattering media, such as biological tissue. Here, we present a method for rapidly acquiring multispectral SFDI data by modulating each illumination wavelength at a different temporal frequency. In the remitted signal, each wavelength is temporally demodulated and processed using conventional SFDI techniques. We demonstrate a proof-of-concept system capable of acquiring wide-field maps (2048×1536 pixels, 8.5×6.4 cm) of optical properties at three wavelengths in under 2.5 s. Data acquired by this method show a good agreement with a commercial SFDI imaging system (with an average error of 13% in absorption and 8% in scattering). Additionally, we show that this strategy is insensitive to ambient lighting conditions, making it more practical for clinical translation. In the future, this technique could be expanded to tens or hundreds of wavelengths without increasing acquisition time. [DOI: 10.1117/1.JBO.22.7.076019]

Keywords: diffuse optics; wide-field imaging; spatial frequency domain imaging.

Paper 170345R received May 27, 2017; accepted for publication Jul. 14, 2017; published online Jul. 31, 2017.

1 Introduction

At near-infrared wavelengths, biological tissue is highly scattering, making high-resolution images of tissue difficult at depths greater than about 1 mm.[1] However, multiply scattered photons carry information about the absorption coefficient (μ_a) and the reduced scattering coefficient (μ_s'), which can reveal the function and structure of the sample. From these optical properties, the concentration of biologically relevant chromophores, such as oxy- and deoxyhemoglobin, lipid, and water, can be deduced. Knowledge of these chromophore concentrations provides a wealth of information about the composition and metabolic activity of tissue, which has proven useful in oncology,[2,3] small animal imaging,[4] exercise physiology,[5] and imaging the brain.[6,7] Most diffuse optics techniques use point-by-point scanning to build up a map of tissue optical properties, but this strategy limits the area and resolution with which tissue can be probed in a clinically relevant period of time.[8] Efforts to increase speed and resolution of point-by-point systems typically involve increasing the number of sources and detectors (often into the hundreds), resulting in devices that are expensive, bulky, and specific to particular anatomical sites.[9,10] Recently, a new technique called spatial frequency domain imaging (SFDI) has been shown to provide wide-field determinations of optical properties of scattering media without point-by-point scanning.[11,12] SFDI involves the illumination of tissue with spatially modulated light and the recording of diffuse reflectance remitted by the tissue using a camera. The response of the tissue in the spatial frequency domain can be related to the spatial domain by an inverse Fourier transform, resulting in 2-D maps of the diffuse reflectance. The resulting reflectance maps can then be used to determine optical properties at each pixel of the image.

*Address all correspondence to: Darren Roblyer, E-mail: roblyer@bu.edu

The first described SFDI processing technique used a minimum of six image acquisitions per wavelength. At each of at least two spatial frequencies, images of the sample were acquired with three spatially offset phases, which were demodulated to obtain the envelope of the diffusely reflected light.[12] This envelope contains information about the structure and composition of the tissue under investigation. During demodulation, DC background illumination is subtracted from the resulting images, rendering this technique theoretically insensitive to ambient light so long as it remains constant during the acquisition. However, the collection of multiple images, as well as the time needed to switch between wavelengths, results in acquisitions times that typically stretch into the tens of seconds. Recently, more advanced demodulation techniques have reduced the number of images needed to two per wavelength,[13] or one per wavelength in a technique termed "single-shot optical properties" (SSOP).[14,15] This method exploits the fact that sinusoidal patterns of light contain at least two spatial frequencies: the DC offset with a spatial frequency of 0 and the AC component at the projected spatial frequency. Low-pass filtering of the image effectively separates out the DC component, while the envelope of the higher frequency component can be computed using a Hilbert transform, or other single-sideband demodulation technique.[16] The single-shot processing method reduces the number of images that need to be acquired at each wavelength from six to one, but still requires that each wavelength be collected sequentially. Furthermore, this technique is more sensitive to changes in ambient light than the original method, posing a challenge for fast-paced clinical environments, where lighting conditions may be constantly changing.

Here, we present a new SFDI acquisition method that enables the rapid collection of optical properties simultaneously from a large number of wavelengths while being insensitive to ambient light. The method borrows from a technique previously used to

enhance hyperspectral fluorescence imaging speed by modulating each excitation wavelength at different temporal rates.[17] In this study, we use three wavelengths of light that are temporally modulated at different frequencies and then used to project a single sinusoidal illumination pattern. We call this method "temporally modulated SFDI" (TM-SFDI). By collecting a sequence of images of the sample while it is illuminated with time-varying light, each pixel of the video can be temporally demodulated by determining the strength of the reflected signal at each modulation frequency. The result of temporal demodulation is a single spatially modulated image at each wavelength, which can then be processed using the SSOP method. Because this technique is only sensitive to light modulated at a specific frequency, it automatically rejects ambient light, unlike conventional single-shot processing. Additionally, because there is no need to switch between wavelengths or projection patterns, acquisition speeds are only limited by the frame rate of the camera and the number of video frames needed for successful temporal demodulation. In Sec. 2, we will describe how the TM-SFDI system was realized; Sec. 3 demonstrates that it is capable of accurately determining optical properties, is insensitive to ambient light, and can be used to image complex samples.

2 Materials and Methods

2.1 *Hardware*

For this proof-of-concept system, three wavelengths of light were used: 519, 652, and 740 nm. One high-power LED per wavelength (Cree XLamp, Cree, Inc. Durham, North Carolina) was driven at 700 mA (652 and 740 nm) or 1000 mA (519 nm) with independent constant current sources. Light from the LEDs was modulated in time using a pulse-width modulation sequence controlled by a microcontroller (Arduino UNO). Modulation frequencies were set at 5.21, 8.68, and 12.15 Hz, each of which falls into a single bin of a 32 point discrete Fourier transform when a sampling period of 18 ms (55.6 frames/s) is used. Frequencies occupying a single bin were important for reducing cross-talk between wavelengths. These frequencies were also chosen to avoid harmonic content from lower frequencies influencing higher frequency modulation. Light from the LEDs was roughly collimated by a lens over each emitter and sent through a transparency printed with a sine wave pattern using a laser jet printer [Fig. 1(a)]. The spatiotemporally modulated light was directed onto a sample, and the reflected light was recorded by a 16 bit scientific CCD camera (Zyla 4.2, Andor, Inc.) with an 8.5×6.4 cm field-of-view (FoV). Crossed polarizers were used to minimize the effect of specular reflection. Modulation and acquisition timings were controlled by a custom Arduino program.

2.2 *Processing*

Videos of temporally modulated light reflected from the sample were acquired at 55.6 frames/s for 2.3 s (128 frames) for offline processing. A Fourier transform in time of each pixel of the image was performed to separate the wavelengths. The amplitude of the spectrum at each modulation frequency corresponded to the intensity of the light reflected by that specific wavelength at that specific spatial location [Fig. 1(b)]. Recording the strength of the peaks at each pixel effectively separates each wavelength, while simultaneously rejecting background light (Fig. 2). Once an image of each wavelength was extracted, the images were rotated to ensure that the stripes were parallel to the top and bottom of the frame, and the optical properties were determined by previously published techniques.[14] Briefly, each image was split into a DC and AC component by taking a spatial Fourier transform of each line of the image and filtering in the spatial frequency domain. The DC image was generated by removing a band of frequencies surrounding the projected AC frequency, leaving the high and low frequency content intact. The inverse Fourier transform of this spectrum was used to determine the diffuse reflectance of the sample under planar illumination. The AC image was

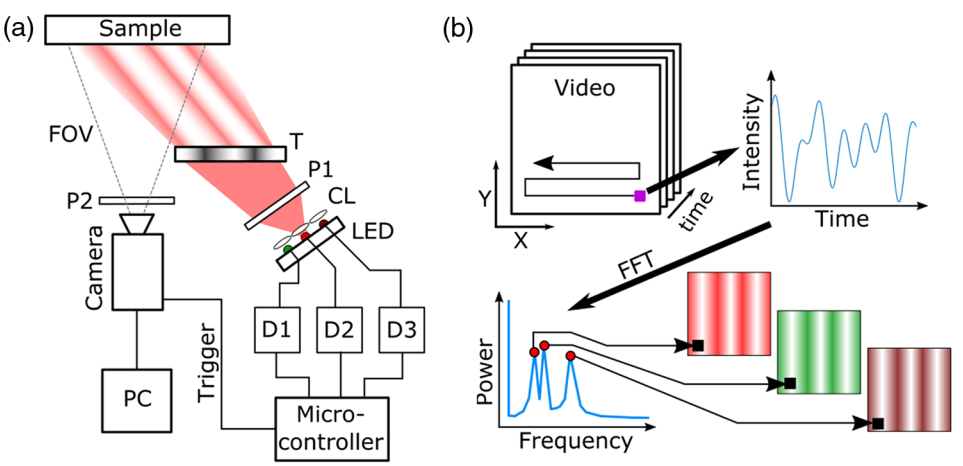

Fig. 1 (a) System diagram. Three LEDs were driven by independent constant current sources (D1, D2, D3) and were temporally modulated by a microcontroller. The light was roughly collimated by three lenses (CL) and polarized (P1) before passing through a patterned transparency (T). Before being imaged by the camera, reflected light passed through a second polarizer (P2) set at 90 deg to P1 to reject specular reflection. Camera FoV is indicated by dashed lines. (b) Schematic of data processing. A video was captured from the camera and the variation of each pixel in time was plotted. An FFT of this time series was taken and the strength of the signal at the frequencies corresponding to the modulation of the LEDs was used to build up a 2-D image for each wavelength. These temporally demodulated images were then processed using the SSOP technique as in Ref. 14.

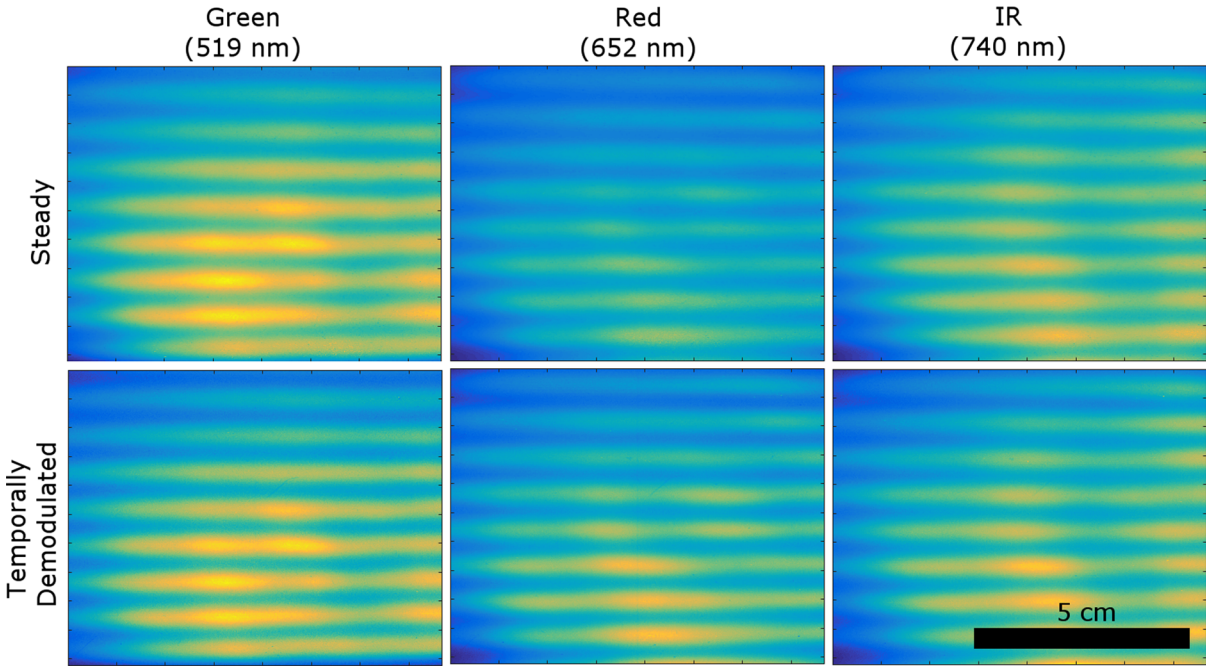

Fig. 2 Comparison of normalized images taken of the spatial pattern when the LEDs were individually illuminated without temporal modulation (top row) versus temporally demodulated images of each wavelength using the TM-SFDI system (bottom row). The images closely match, showing the ability of temporal demodulation to separate different wavelengths. The scale bar applies to all images.

obtained via Hilbert transform followed by inverse Fourier transform of the high frequency content. The demodulated AC and DC images were compared with a reference standard to obtain the calibrated reflectance of each pixel in the image. Optical properties were calculated by interpolating a look-up table relating calibrated reflectance values to optical properties, which was generated by scaling of a single Monte Carlo simulation.[12,18]

2.3 *Accuracy and Drift*

To test the accuracy of the TM-SFDI system, a set of 13 tissue mimicking phantoms with varying optical properties were imaged three times over 3 days with a commercial SFDI system (OxImager RS, Modulated Imaging, Inc.) at wavelengths of 526, 659, and 729 nm to establish the "gold standard" measurements of the phantom optical properties. The same set of phantoms was also imaged three times over 3 days with the TM-SFDI system at wavelengths of 519, 652, and 740 nm. Both systems used measurements of a reference standard with known optical properties for instrument response calibration. To account for variability in the TM-SFDI system, the reference standard was imaged five times per day and the temporally demodulated images were averaged together before being used to calculate μ_a and μ_s' at each wavelength. Optical properties of the phantoms from both the commercial system and the TM-SFDI system were calculated using the same SSOP algorithm and compared against each other. Because the same wavelengths were not available for both systems, a correction factor was implemented to estimate the optical properties calculated by the commercial system at the wavelengths used in the TM-SFDI system. To construct the correction factor for μ_a, the absorption spectrum of nigrosin, the chromophore used to make the tissue mimicking phantoms, was measured using a spectrophotometer. The correction factor for absorption was defined as $\mu_a(\lambda_{TM}) = \frac{\mu_a(\lambda_{Com})\epsilon(\lambda_{TM})}{\epsilon(\lambda_{Com})}$, where $\mu_a(\lambda_{TM})$ is the estimated absorption coefficient at the TM-SFDI wavelength λ_{TM}, $\mu_a(\lambda_{Com})$ is the measured absorption coefficient at the wavelength of the commercial system (λ_{Com}), and $\epsilon(\lambda)$ is the extinction coefficient of nigrosin at the wavelength λ measured with the spectrophotometer. To estimate how μ_s' changes with wavelength, we assumed a Rayleigh scattering ($\mu_s' \propto \lambda^{-4}$) relationship and defined the correction factor as $\mu_s'(\lambda_{TM}) = \frac{\mu_s'(\lambda_{Com})\lambda_{Com}^{-4}}{\lambda_{TM}^{-4}}$, where $\mu_s'(\lambda_{Com})$ is the reduced scattering coefficient calculated by the commercial system at λ_{Com}. Rayleigh scattering was assumed because scattering in the phantoms is controlled by altering the concentration of titanium dioxide nanoparticles, the diameters of which are much smaller than the wavelengths of light used. The maximum change in optical properties using these correction factors was slightly over 5%. Each TM-SFDI scan consisted of 128 2048×1536 pixel images, with an FoV of 8.5×6.4 cm. To improve the signal-to-noise ratio, the temporally demodulated images were downsampled using 2×2 averaging.

To assess the stability of the TM-SFDI system, a single tissue mimicking phantom was scanned every 10 min for 2 h following a 30-min warm up period, and the variations in calibrated reflectance and optical properties at each wavelength over that time were calculated based on comparison with a reference standard imaged at the start and end of the drift test. Each scan consisted of 128 images.

2.4 *Effect of Ambient Light*

To test the effect of ambient light on TM-SFDI, a calibration phantom was imaged in complete darkness. TM-SFDI videos were then acquired at various levels of ambient light controlled

by changing the distance between the bulb of a standard desk lamp and the sample. Images of a single wavelength not modulated in time were also acquired to compare the TM-SFDI technique with the SSOP method.

3 Results and Discussion

3.1 *Accuracy*

We found that there was a good agreement in optical property extractions between the gold standard commercial instrument and the proof-of-concept TM-SFDI system (Fig. 3). The average error in absorption between the TM-SFDI and the gold standard was 13%. The TM-SFDI system was more accurate at extracting reduced scattering, with an average error of 8% compared with the gold standard. The absorption measurements were biased, consistently underestimating the actual absorption coefficient by an average of 0.003 mm^{-1}, while the scattering measurements were biased in the other direction, overestimating μ_s' by an average of 0.088 mm^{-1}.

In addition to homogeneous phantoms, a more complex tissue simulating phantom was imaged. The sample was a 3-D printed block of acrylonitrile butadiene styrene that featured a network of vascular like channels filled with a highly absorbing acrylic copolymer (P400SR, Stratasis, Inc.). The complex phantom was imaged with the TM-SFDI system, and a good correlation between the printed channel and the absorption map was noted (Fig. 4).

3.2 *Drift*

The drift of the TM-SFDI system was tested by allowing the system to warm up for 30 min and then repeatedly measuring the same phantom every 10 min for 2 h. The average changes in calibrated reflectance over this time period were less than 3% for the AC and DC components. However, these errors translated into a relatively large average variation in μ_a of 13% about the mean. The average variation in μ_s' was 1%. There was no systematic rise or fall to the change but rather a random variation about the mean. To determine the source of the drift, we tested each LED individually with DC illumination and no temporal modulation and found a variation of 1% to 3% of output intensity over time. Though relatively small, this variation would also change the calibrated reflectance by the same 1% to 3%, which maps to a greater than 10% change in μ_a. The observed variation in optical properties is likely due to instability of the LEDs and driver electronics, which were both consumer grade. We expect that upgrading these components and implementing temperature control would reduce the variability in measured optical properties.

3.3 *Effect of Ambient Light*

We found that the TM-SFDI system was almost entirely insensitive to the ambient light level. In Fig. 5, the calibrated reflectance for planar illumination is shown for SSOP (blue) and TM-SFDI (red) along with linear fits to the data at a variety of ambient light levels. The slope of the linear fit of the TM-SFDI DC reflectance was not significantly different from zero ($p = 0.5$) using a two sided t-test, indicating that there was no relationship between ambient light level and calibrated reflectance. The change in calibrated reflectance using SSOP would result in extremely large errors in optical properties as ambient illumination changed. Future instruments using TM-SFDI will need to avoid frequencies near the AC power supply (typically 50 or 60 Hz) to avoid contamination from the flickering of room lights.

3.4 *Discussion*

The TM-SFDI system presented here allows for the rapid acquisition of diffuse optical images. At 56 frames/s and a typical video length of 128 frames, we were able to capture spectroscopic images of optical properties at three wavelengths in 2.3 s. The number of simultaneous wavelengths that can be collected is limited by the number of video frames acquired. The

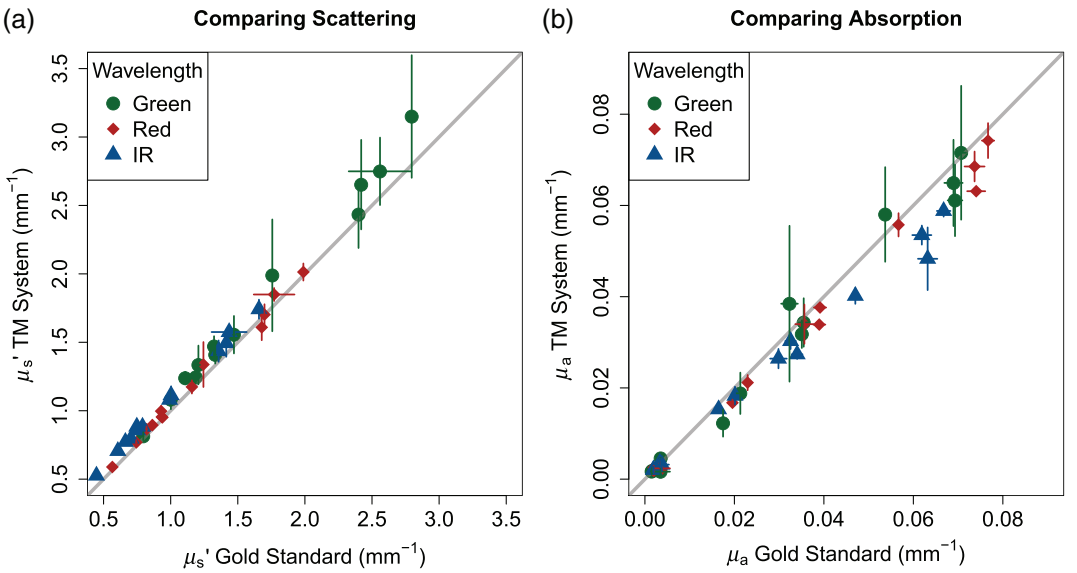

Fig. 3 Comparison of TM-SFDI with gold standard in terms of (a) scattering and (b) absorption. The identity line is shown in gray. Error bars indicate ±1 standard deviation of the average measured optical property across the 3 days. Acquisition time was 2.3 s for the TM system versus ~30 s for the gold standard device.

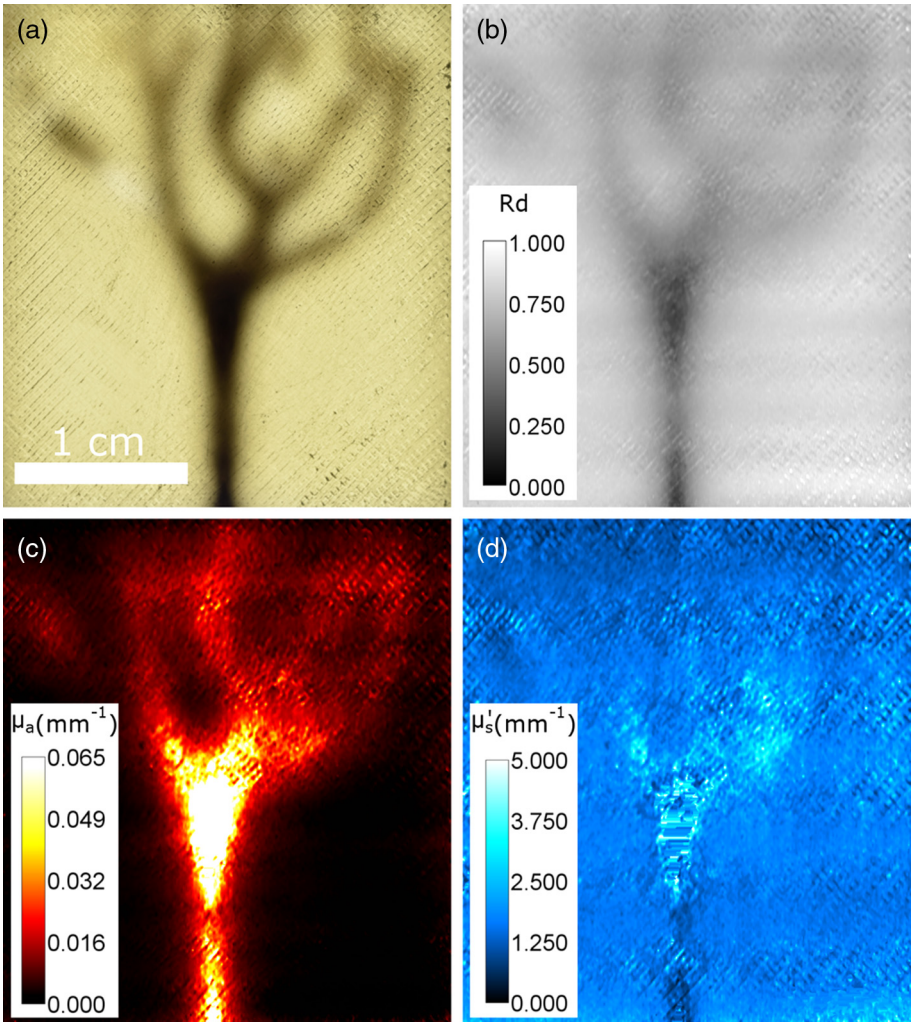

Fig. 4 (a) Photograph of the 3-D printed phantom with vessel-like inclusions under strong back illumination. (b) Temporally and spatially demodulated image of calibrated DC reflectance at 652 nm. (c) Map of the absorption coefficient and (d) map of the reduced scattering coefficient of the sample (d) at 652 nm. Scale bar applies to all images. Median filtering was used on panels (c) and (d) to remove artifacts.

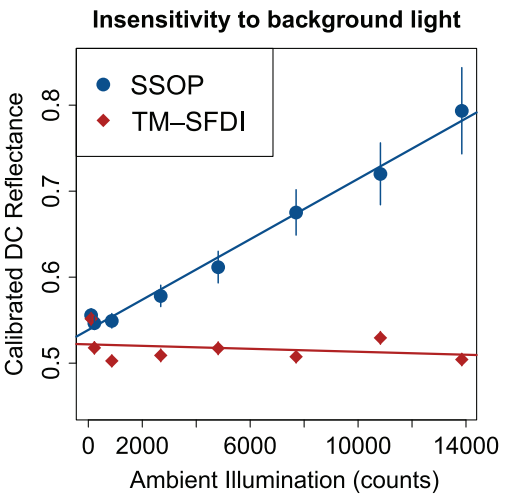

Fig. 5 Temporally modulated (blue) SFDI compared with single shot SFDI (red) under varying levels of ambient light. TM-SFDI is largely insensitive to the ambient light level while SSOP is highly sensitive. Error bars represent ±1 standard deviation of the pixels in the image.

maximum number of wavelengths that can be unambiguously demodulated is no more than one per FFT bin (excluding DC). This means that a 128 frame scan could theoretically support 63 wavelengths, while a 256 frame scan could support 127, although practically, this number of wavelengths may be reduced due to spectral leakage. We experimented with using fewer video frames (64, 32, 16, etc.) and found an increased scan-to-scan variability. Using 64 images, there were only modestly higher errors (10% in scattering and 24% in absorption), meaning acquisition speeds of around 1 s with reasonable errors are possible. Since the maximum frame rate of the camera increases when fewer CCD lines need to be read, using a smaller FoV could also increase acquisition speed. For an image of 512×512 pixels, it would be possible to increase the frame rate from 55.6 to 80 fps, resulting in a minimum acquisition time of 800 ms for up to 16 wavelengths.

Recent work has utilized a similar temporal modulation of excitation wavelengths for single pixel SFDI.[19] Despite advantages in simplicity of hardware, cost, and bandwidth, single pixel imaging scales poorly with resolution, requiring the projection of over 31,000 patterns for each spatial frequency and

phase to acquire an image with a comparable number of pixels used in this study. For example, Torabzadeh et al.[19] used single-pixel SFDI to acquire 400 samples in 80 ms, meaning a single high resolution image could be collected every 6.2 s. While a large number of pixels is not strictly necessary for low-resolution diffuse imaging, it allows for pixel binning to reduce the overall noise level. Greater numbers of pixels would also allow for the possibility of imaging larger FoVs without impacting resolution.

The TM-SFDI system has several limitations worth noting. The first is variability in μ_a extractions. The errors in absorption are likely due to the fact that, at the chosen spatial frequencies, small changes in reflectance map to large changes in μ_a, meaning that the effects of noise and LED instability are amplified.[4] It is likely that temperature variations of the LEDs and driver circuit led to instability of the LED output and resulted in uncertainty in the absorption estimates. We also found that the estimates for optical properties were biased with the absorption being underestimated and the scattering overestimated. We believe both biases are due to broadband noise contaminating the images, resulting in small, systematic errors in diffuse reflectance as well as nonlinearities in system response, which are not accounted for in the calibration step and result in increased errors for samples with optical properties that differ significantly from the calibration phantom. It is likely that improvements in the signal-to-noise ratio and careful choice of calibration phantom will help resolve this issue. Second, the acquisition time of 1 to 2 is relatively long compared with the SSOP method, and the sample must be held motionless for that entire time to achieve a clear image of the resulting optical properties. This could potentially be solved by adding an image registration step to align the frames of the video prior to processing. Third, although scans can be performed relatively quickly, processing of the data requires significant computational resources. Each scan requires over 300,000 FFTs to be performed as well as searching a nonlinear look-up-table for each pixel at each wavelength. On a relatively modern desktop computer (Intel i7-6700, 16 GB RAM), the time to process each scan was about 80 s. However, much of the processing is parallelizable and could likely be vastly sped up by offloading to a graphics processing unit.

4 Conclusion

In conclusion, we have constructed a high-speed SFDI system that enables the acquisition of spectrally resolved optical properties without needing to switch between illumination patterns or wavelengths. Currently, the system operates at ~750 ms/wavelength, but, since acquisition time does not scale with the number of wavelengths used, this could be increased to ~50 ms/wavelength by adding additional illumination wavelengths. By mapping the spectral components of light into the time domain, this system eliminates the need to acquire each wavelength sequentially. Importantly, the temporal modulation of light also makes this system insensitive to background illumination, making it a practical technique for translation into the clinic, where light levels vary widely and cannot easily be controlled. Future work will investigate increasing the stability of the LEDs, increasing the number of modulated wavelengths using dispersed supercontinuum light in conjunction with a linear spatial light modulator, testing the TM-SFDI on a variety of biological samples, and including single-shot height correction for more accurate imaging of 3-D samples.[15]

Disclosures

The authors have no conflicts of interest to disclose.

Acknowledgments

The authors gratefully acknowledge funding from the U.S. Department of Defense (DoD) (Award No. W81XWH-15-1-0070).

References

1. W. R. Zipfel et al., "Live tissue intrinsic emission microscopy using multiphoton-excited native fluorescence and second harmonic generation," *Proc. Natl. Acad. Sci. U. S. A.* **100**, 7075–7080 (2003).
2. D. Roblyer et al., "Optical imaging of breast cancer oxyhemoglobin flare correlates with neoadjuvant chemotherapy response one day after starting treatment," *Proc. Natl. Acad. Sci. U. S. A.* **108**, 14626–14631 (2011).
3. P. G. Anderson et al., "Broadband optical mammography: chromophore concentration and hemoglobin saturation contrast in breast cancer," *PLoS One* **10**(3), e0117322 (2015).
4. S. Tabassum et al., "Feasibility of spatial frequency domain imaging (SFDI) for optically characterizing a preclinical oncology model," *Biomed. Opt. Express* **7**(10), 4154–4170 (2016).
5. T. Hamaoka et al., "The use of muscle near-infrared spectroscopy in sport, health and medical sciences: recent developments," *Philos. Trans. R. Soc. A* **369**(1955), 4591–4604 (2011).
6. A. V. Medvedev et al., ""Seeing" electroencephalogram through the skull: imaging prefrontal cortex with fast optical signal," *J. Biomed. Opt.* **15**(6), 061702 (2010).
7. D. A. Boas et al., "The accuracy of near infrared spectroscopy and imaging during focal changes in cerebral hemodynamics," *Neuroimage* **13**(1), 76–90 (2001).
8. F. Bevilacqua et al., "Broadband absorption spectroscopy in turbid media by combined frequency-domain and steady-state methods," *Appl. Opt.* **39**, 6498–6507 (2000).
9. C. Li et al., "Multispectral breast imaging using a ten-wavelength, 64×64 source/detector channels silicon photodiode-based diffuse optical tomography system," *Med. Phys.* **33**(3), 627–636 (2006).
10. A. T. Eggebrecht et al., "Mapping distributed brain function and networks with diffuse optical tomography.," *Nat. photonics* **8**(6), 448–454 (2014).
11. N. Dögnitz and G. Wagnières, "Determination of tissue optical properties by steady-state spatial frequency-domain reflectometry," *Lasers Med. Sci.* **13**(1), 55–65 (1998).
12. D. J. Cuccia et al., "Quantitation and mapping of tissue optical properties using modulated imaging," *J. Biomed. Opt.* **14**(2), 024012 (2009).
13. K. P. Nadeau, A. J. Durkin, and B. J. Tromberg, "Advanced demodulation technique for the extraction of tissue optical properties and structural orientation contrast in the spatial frequency domain," *J. Biomed. Opt.* **19**(5), 056013 (2014).
14. J. Vervandier and S. Gioux, "Single snapshot imaging of optical properties," *Biomed. Opt. Express* **4**(12), 2938–2944 (2013).
15. M. van de Giessen, J. P. Angelo, and S. Gioux, "Real-time, profile-corrected single snapshot imaging of optical properties," *Biomed. Opt. Express* **6**(10), 4051 (2015).
16. S. L. Hahn, *Hilbert Transforms in Signal Processing*, Vol. **2**, Artech House, Boston (1996).
17. S. R. Domingue, D. G. Winters, and R. A. Bartels, "Hyperspectral imaging via labeled excitation light and background-free absorption spectroscopy," *Optica* **2**(11), 929 (2015).
18. M. Martinelli et al., "Analysis of single Monte Carlo methods for prediction of reflectance from turbid media," *Opt. Express* **19**(20), 19627 (2011).
19. M. Torabzadeh et al., "Compressed single pixel imaging in the spatial frequency domain," *J. Biomed. Opt.* **22**(3), 030501 (2017).

Matthew B. Applegate is a postdoctoral researcher in the Department of Biomedical Engineering at Boston University. He received his BS in electrical engineering from Cornell University in

2009 and his PhD in biomedical engineering from Tufts University in 2016. His current research interests are focused on developing new, clinically translatable optical techniques using diffuse optics, OCT, and nonlinear optics.

Darren Roblyer is an assistant professor in the Department of Biomedical Engineering at Boston University. After receiving his BS degree in biomedical engineering from Johns Hopkins University in 2004, he received his PhD as a HHMI Med-Into-Grad Fellow in 2009 from the Bioengineering Department at Rice University, where he studied under Rebecca Richards-Kortum. Prior to starting his faculty position in 2012, he was a postdoctoral fellow at the Beckman Laser Institute studying under professor Bruce Tromberg.